CrossMark

ORIGINAL PAPER

The Inhibitory Effect of Magnesium Sulfonate as a Fuel Additive on Hot Corrosion of Generating Tubes of Power Plant Boiler

Mohamad Sadegh Amiri Kerahroodi[1] · Khosrow Rahmani[1] ·
Masoud Yousefi[1]

Abstract Changing the power plant boiler fuel from natural gas into fuel oil during the cold months of the year causes hot corrosion in generating tubes. Visual observations, thickness and thermocouple measurements and ash analysis proved the hot corrosion by displaying the sticky melted ash, thickness reduction, surface temperature of tubes at about 600 °C and existence of complex corrosive elements such as sodium and vanadium, respectively. Therefore, based on the experimental data from the power plant, laboratory studies were performed to survey the corrosion inhibition effect of magnesium sulfonate as an easy to use fuel additive. A low carbon steel, 70 wt%Na_2SO_4–25 wt%V_2O_5–5 wt%NaCl and mineral part of magnesium sulfonate ash were used as the generating tube material, corrosive and additive ashes, respectively. Two groups of specimens were coated with two different compounds of synthetic ashes, in which the first group was containing corrosive salts and the second was a calculated specific combination of mineral part of additive ash and corrosive salts. Specimens were exposed to high temperatures up to 120 h at 600 °C. Power plant observations, XRF, weight loss criteria, SEM and FESEM were used to study the hot corrosion, and results were compared with similar studies. It was concluded that magnesium sulfonate could not attribute to reduce the emission of sulphurous gases. Although the first group of the specimens was highly suffered from corrosion, the other group of samples was protected against hot corrosion and the weight loss was decreased considerably. Morphology and XRD picks of corrosion products were described, and it was also concluded that $Na_4V_2O_7$ and NaV_3O_8 compounds which are molten at 600 °C were responsible for hot corrosion. The additive inhibited corrosion through formation of Na_3VO_4 with

✉ Mohamad Sadegh Amiri Kerahroodi
sadeghamiri@aol.com

[1] Energy and Mechanical Engineering Department, Abbaspour-Power and Water- College of Engineering, Shahid Beheshti University, P.O. Box. 16765-1719, Tehran, Iran

850 °C melting point and prevented the formation of sticky and corrosive compounds.

Introduction

When the surface of the metals and alloys are covered by molten salts in existence of oxidizing gas at high temperatures, they experience an accelerated corrosion that is called high temperature or "hot" corrosion [1, 2]. The rising in the usage of the liquid fuel derived from petroleum causes the decrease in quality of residual oils that are becoming heavier. Hence, an increase in the level of vanadium, sodium and sulfur in chemical compound of liquid petroleum that is usually used in power plant boilers, has been detected [3]. Ash fouling and fire side corrosion on the surface of the metals, along with heat transfer of fouling surface, are important problems in power plants when heavy fuel oils [4] are specially used in steam generation equipment (boiler) at high temperatures (600–1100 °C) [5]. Fire side corrosion is generally occurred in two sections [6]:

1. Beneath deposit of furnace wall evaporator tubes.
2. Beneath deposit corrosion of reheater and superheater tubes and the upper end of the furnace chamber and in the convection pass [7].

Hot corrosion is principally the result of attack during combustion and ash products such as Na, V, S, Cl, and it depends on the combustion and ash concentration created during combustion of fuel oil [3, 8]. V_2O_5, Na_2SO_4 (from fuel) and NaCl (from air) are the main parts of fuel oil ash corrosion. The existence of Na_2SO_4 accelerates the corrosion rate through the fluxing of protected oxide formed on the metal surface or by adding sulfur which makes the oxide scale non-protective. Vanadium pentoxide and alkali metal trisulfides in ash react to create low melting point scales that flux the protective oxide scale on the surface of metal and cause the accelerated corrosion attack [9]. Vanadium products are extremely corrosive and are stable under the normal operating conditions of boiler [5] and react with scales in combustion gases and presence of oxygen and form the low melting point vanadate which causes the fluxing reactions as a result of accelerated corrosion [6]. The reaction between vanadium and sodium sulfate leads to the formation of vanadate compound as $V_2O_5 + Na_2SO_4$ low melting point (600 °C). According to the Reid studies, a compound containing 20% V_2O_5 and 80% Na_2SO_4 melts at 320 °C, whereas a product containing 40% V_2O_5 and 60% Na_2SO_4 has a melting point of 550 °C. This means that a mixture of V_2O_5–Na_2SO_4 which has 20–40% of V_2O_5 could form products with low melting points [9]. Sodium vanadyl vanadate is the most prevalent compound found on boiler superheaters, which has a low melting point at about 550 °C [2, 10]. However, most of the mechanisms are related to fluxing of the protective oxide or reaction with special salt compounds.

Depending on the salt composition, oxides may dissolve in Na_2SO_4 as anionic species (basic fluxing) or cationic species (acid fluxing) [11]. V_2O_5 can react with Na_2SO_4 to increase the acidity of the melt via the following reaction [12]:

$$V_2O_5 + Na_2SO_4 \rightarrow 2NaVO_3 + SO_3 \qquad (1)$$
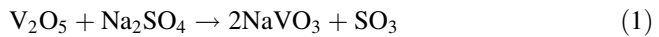
Due to the high expenses of fuel refining from these impurities, the consumption of low grade fuels is generally justified [13]. Solving of the oil ash corrosion problem is associated with controlling the critical factors that govern it. One of the efficient ways is injecting additives (high melting point compounds) into the fuel to increase the melting point of the deposited ash. Effective additives are the compounds of magnesium, calcium, and barium. The additives react with vanadium compounds to create reaction products with higher melting points [9].

The effect of magnesium compounds is to form the compounds with melting points higher than 600 °C such as $MgO \cdot V_2O_5$ (m.p = 671 °C), $2MgO \cdot V_2O_5$ (m.p = 835 °C) and $3MgO \cdot V_2O_5$ (m.p = 1191 °C) from vanadate [9]. For ordinary applications, a minimum 3–1 weight ratio of magnesium-to-vanadium (Mg/V) is recommended. There are three typical sorts of magnesium-based additives: water-soluble, oil-soluble and oil dispersible. Magnesium sulfate (Epsom salt) is the water-soluble additive. It is used as a 10 to 20% water solution of magnesium sulfate which must be emulsified into the fuel. Since it does not form a stable emulsion in the fuel, the solution must be injected into the fuel just in prior to use. Oil-soluble inhibitors are proprietary products which blend readily and uniformly in the fuel to form stable mixtures. Oil-dispersible inhibitors are stable suspensions of very finely divided solid magnesium compounds. They are outgrowths of "fireside" additives used in boilers for corrosion and ash deposit control. Oil-dispersible inhibitors form stable mixtures in the fuel if some mixing is provided [14].

In some countries, power plants change the boiler fuel from natural gas into fuel oil during the winter for a short period of time, in order to be sure about supplying the urban needs of natural gas. Those changes cause lots of problems during the winter such as higher air pollution and hot corrosion in some parts of boilers. Based on power plant observations and technical reports, experimental tests were performed to offer a solution for hot corrosion that leads to replace generating tubes and stop the production. In this study using magnesium sulfonate was suggested for power plant and its inhibition effect was surveyed.

Experimental Procedures

System Description

The Besat power plant is located in the south of Tehran (the capital of Iran) and has three 82.5 Mw units that were made by general electric company in 1968. The main fuel was natural gas, and the fuel oil was used for a few months in year during the winter. The boilers are natural circulation type with under pressure furnace in which

the entrance steam flow through turbine is 790,000 lb/h with 1250 psi pressure at 510 °C.

Boiler is one of the main parts of the power plant that is responsible for changing water to superheat steam. Natural gas and fuel oils are the principal fuels that are used in the Middle East power plants. The thermal energy from combustion of those fuels heats the water that is preheated in the water wall tubes and converts it to vapor. The steam contains some water that is separated in drum and goes throughout superheater tubes and turbine. The dry steam after a few stages in turbine goes into condenser and it is reused again in this cycle [15]. The water (separated from drum) reaches to condenser throughout downcomer tubes, and then it is divided into water wall tubes. In some power plants like the current case, water transfers from the upper drum into the lower drum throughout generating tubes and then the water distribution is done. The lower drum acts as a header. The boiler has two drums. There was hot corrosion problem with generating tubes when the fuel was changed from natural gas into fuel oil. Therefore, further tests were performed:

1. Visual inspection.
2. NDT tests for generating thicknesses of tubes.
3. Temperature measurements of tube surface by thermocouples.
4. Ash XRF analysis of tube surface.

Raw Materials

Material Properties of Specimen

Power plant design is based on concepts such as water wall tubes which need very little refractory elements, since the water goes through the tubes and cooling effect of water prevents thermal damages. When the mean temperature is around 427 °C and boiler is properly operated, carbon steels can be used [15]. Due to the inappropriate operation, the temperature in generating tubes that are made by carbon steels can be increased up to 600 °C which causes failure. In this case, in order to understand the high-temperature corrosion behavior of the generating tubes, plain carbon steel was selected to be studied in synthetic ash. The measured chemical composition of the generating tubes (low carbon steel) is shown in Table 1. Rectangular sheets of the plain carbon steel were cut with 25 × 15 × 1.5 mm dimensions as the test specimens.

Table 1 Chemical composition of low carbon (St-37) steel (wt%)

Element	Cu	Mo	Ni	Cr	S	P	Mn	Si	C
%	0.03	0.002	0.02	0.01	0.006	0.012	0.60	0.01	0.12
Element	Fe	Zr	V	Sb	As	Sn	Al	Co	Ti
%	Base	Trace	0.003	0.002	0.002	0.01	0.05	0.005	0.001

Corrosive Compound

The chemical compound of corrosive salt was selected after evaluation of power plant ash analysis in Table 2. The corrosive compound was a mixture of 70 wt% Na_2SO_4, 25 wt% V_2O_5 and 5 wt% NaCl. It must be noticed that Table 2 is described ash XRF analysis of the tube surface section with more details.

Chemical Analysis of the Additive Ash

Among organometallic additives, overbased magnesium sulfonate was made as an inhibitor through patent description [16]. Overbased magnesium sulfonate is the highly saturated (12 wt% Mg) solution (brawn liquid) of magnesium (oxide or carbonate) in alkylbenzene sulfonic acid that can be added directly to the fuel oil without special equipment. As it is shown in Fig. 1, magnesium ion has been solved in a dodecylbenzene sulfonic acid (as a alkylbenzene sulfonic acid); therefore, the entire compound in Fig. 1 is magnesium dodecylbenzenesulfonate and the circled part is magnesium sulfonate with MgO_3S molecular form but it is commercial to call the whole of compound, magnesium sulfonate. It must be noticed, some impurities in the fuel oil such as vanadium are generally present in the form of porphyrins or asphaltenes [17] but when they burn and deposit on the surface of tubes, they convert into a mineral form like, V_2O_5. Furthermore, some parts of corrosive salt come from the air like NaCl [9] and all the ashes from different sources react with each other in mineral form on the surface of tubes. Consequently, the background of ashes is not important. Moreover, the form which contributes to corrosion reactions is mineral part of impurities.

Barbooti et al. [4] used the burned magnesium stearate as ash for their hot corrosion inhabitation tests and mixed this ash with corrosive salts to make Mg-containing compounds. Using mineral for the experiments makes weighing more exact than using ash, because ash contains unburned carbons. In addition, magnesium sulfonate is in liquid state, so it could not be coated on specimens directly. As a result, magnesium sulfonate was burnt similar to the test condition at 600 °C in the air atmosphere. XRD test (JEOL, JDX–3530 M, Czech model) with BS EN 13,925-1:2003 reference standard was done to determine the mineral salt part of additive ash. This mineral compound was selected as the additive ash. As it is shown in Fig. 2, $MgSO_4$ was the only mineral part of the additive ash.

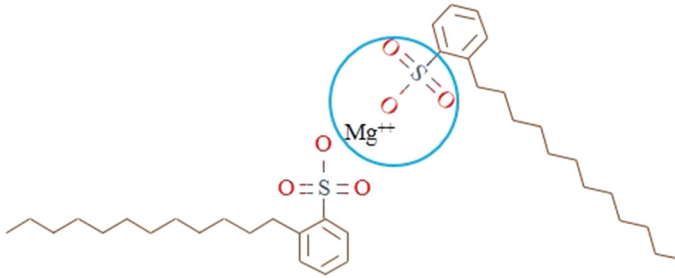| Table 2 Ash XRF analysis of the tube surface					
SiO_2	1.55	Fe_2O_3	7.39	Na_2O	24.89
Al_2O_3	1.46	MnO	0.04	SO_3	28.5
MgO	0.16	CaO	0.85	V_2O_5	19.48
P_2O_5	0.05	K_2O	0.45	L.O.I (CO_2, H_2O)	14.22

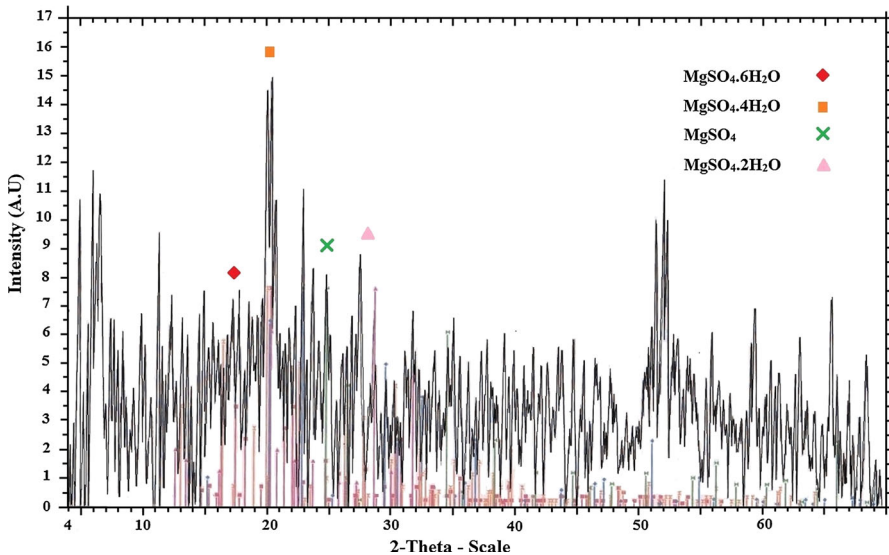**Fig. 1** Structure of magnesium dodecylbenzenesulfonate

Fig. 2 XRD patterns of additive ash after burning at 600 °C

Assessment of Hot Corrosion Resistance

Hot corrosion on the surface of tubes is the result of salts chemical reactions with metal. So, in order to compare the effect of fuel additive on hot corrosion behavior of specimens, two groups of salt mixtures were prepared to coat on specimens. The first type was a corrosive compound, and the second was a mixture of corrosive compound and $MgSO_4$ that was called Mg-containing compound. As mentioned, corrosive compound was a mixture of 70 wt% sodium sulfate (Na_2SO_4), 25 wt% vanadium pentoxide (V_2O_5) and 5 wt% sodium chloride (NaCl). The Mg-containing compound was a mixture of corrosive compound and $MgSO_4$.

Obviously, the amount of Mg in Mg-containing compound has influence on hot corrosion inhibition. Due to this fact, four different Mg-containing compounds were made in that $MgSO_4$ which was added to the corrosive compound until the weight ratio of Mg to V in the compounds reach to 1:1, 2:1, 3:1 and 4:1. Four samples were

coated with four different Mg-containing compounds by further considerations for sample preparing in hot corrosion assessments. The only difference was that the samples were put in the furnace at 600 °C in air atmosphere without bringing out at each 24 h. The Mg compound that had lowest weight loss was selected for further studies such as cyclic hot corrosion studies, XRD and FESEM analysis.

Two groups of specimens were coated with corrosive compound and Mg-containing compound. To create slurry of compounds, distilled water was added to them. To remove all coarse scratches and contaminations, specimens were polished by silicon carbide paper up to 400-grit. Ten Specimens were divided in two groups with five specimens in each group. The first group was coated with corrosive compound and the second with Mg-containing compound. The specimens were rinsed by water and were air-dried. Prior to coat the compounds, specimens were weighed and preheated to 250 °C for 30 min [18]. The weighing was done with milligram accuracy. The slurry coatings were added to the specimens while they were on the heater. Preheating the specimens improves salt adhesion by helping to evaporate water in the slurry. The coated specimens were then weighed to determine the amount of salt applied. This way was repeated to reach the coating weight at about 15 mg/cm^2. After that specimens were heated at 120 °C for 2 h to remove any remaining moisture from the coated specimens. Then, the specimens were again weighed immediately and the weights of coated specimens were recorded. Each coated specimen was put in the alumina boat. Both groups of coated specimens were placed inside the two furnaces maintained at 600 ± 5 °C. The furnace was electrical heat treatment furnace under the air atmosphere. The specimens were held for 24 h at 600 °C. Then, after switching off the furnaces, the specimens were kept in them for 24 h to prevent any thermal shocks. Although the temperature had reached to 50 °C, the specimens were heated at 120 °C for 2 h to remove any remaining moisture before weighing. One specimen was discarded from each group at each cycle. The other specimens were washed with water and dried. In order to show the effect of scale growth on corrosion rate, the washing was done smoothly without removing scales. Then samples were recoated, and this cycle was repeated for five times until the last specimen passed 120 h. It is expected that the washing off the salts without removing the scales would show the effect of oxide scale growth on hot corrosion. It seems this method provide a way for surface defects like pits to growth by preventing surface defects removing and refreshing corrosive salts. Removing scales in each cycle just presents weight loss and does not show any trend in appearances. Hence, there were five discarded specimens for each group. Therefore, there were specimens for 24, 48, 72, 96 and 120 h. Morphological studies were performed for each specimen by FESEM. Moreover, the corrosion products of final specimens for both groups that passed 120 h were examined by XRD analysis. After surface studies, the surfaces of all the specimens were chemically cleaned according to ASTM G1 81 standard [12]. In addition, the weight losses of specimens were calculated. Weight losses were divided to exact area of each specimen to graph the weight and material losses in mg/cm^2 and μm over the time, respectively.

Microstructural Analysis

A FESEM (Make: TESCAN, Czech; Model: Mira 3-XMU) equipped with an EDS was used for studying the microstructure (surface morphology) and chemical compositions of the deposits. For the surface morphological studies of the discarded specimens, the specimens were not washed with distilled water prior to FESEM, EDS and line scan analysis.

Cross-sectional studies of the specimens were performed by scanning electron microscope (Made by: TESCAN, Czech; Model: VEGA LMV) equipped with an EDS.

X-Ray Diffraction Studies

As discussed in assessment of hot corrosion resistance section, two specimens that totally stayed for 120 h in the furnace were selected for XRD experiment. Specimens were subjected to X-ray diffraction (XRD) studies using computerized diffractometer with $CuK_{\alpha 1}$ radiation (0.154 nm) and Ni filter. The XRD data were further analyzed using X'pert high score software to determine the constituent phases.

Results and Discussion

Power Plant Data

Visual Inspection

Visual inspection is one of the most important ways to determine the failure reason of any industrial structure and equipment. The main duty of generating tubes is transferring water from upper drum to the lower drum. The water that enters to the lower drum was distributed in the water wall tubes. Generating tubes were in the path of combustion products after the superheat section. After these tubes, economizer was the next section. Figure 3 shows the location of generating tubes in the boiler.

External tubes (in the direction of economizer and superheater tubes) contain two bents. Tubes in the internal section (Dog house) have bigger bents. The first and the last tubes are conical forms. Depending on the location of tubes, the sizes of tubes were different. Surveying the tubes showed that the external diameter of tubes and the thickness were 76.2 mm and at about 4.6 mm, respectively. In conical sections, the external diameter and the thickness were 55 mm and at nearly 5.6 mm, respectively.

Though the number of damaged tubes in the side of superheater was 73 tubes, only one tube was damaged in the side of economizer. The most damaged tubes were in the direction of furnace or superheater tubes. Figures 4 and 5 display the general view of generating tubes in the side of economizer and super heater,
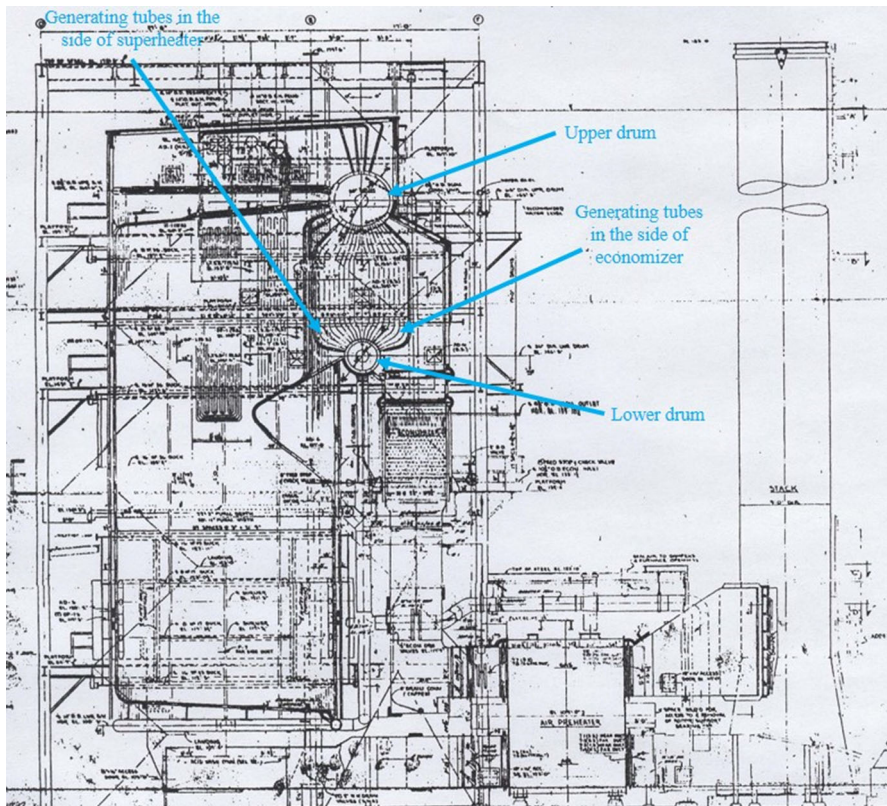
Fig. 3 Location of lower drum and upper drum and the connecting tubes (generating tubes) in the boiler

respectively. As it is shown, it seems that the problem is more related to the outdoors of tubes, because the chemistry of water in the both sides is same.

The closer look on the surface of tube, in the side of the superheater, shows that the combustion products of the fuel oil cause the hot corrosion. In some points, the thickness of deposits was at about 3–4 mm. Due to the shape of the combustion products, it seems that the temperature on the surface of tubes is higher than the standard. There is no sign of corrosion products in the side of economizer. Figure 6 shows the combustion products on the tubes in the side of superheater with sticky ash deposits.

Thickness Measurements

By using non-destructive test during the power plant overhaul, it is possible to determine the condition of the boiler tubes. One of the most important uses of the non-destructive test is forecasting the boiler performance during the operation, changing sensitive tubes and preventing destruction of other equipment. Power plant generating tubes were examined by using the ultrasonic method for measuring the

Fig. 4 Generating tubes in the economizer side

Fig. 5 Generating tubes in the superheater side

thickness. By considering the accessibility of generating tubes in the side of economizer or superheater, eight tubes were randomly selected and their thicknesses were measured. The thickness measurements were performed to determine the thickness in the both smooth and conical section of tubes. Table 3 shows the thickness of tubes in both sides.

As can be seen in Table 3, due to the proper thickness of tubes in the side of economiser, this side of the tubes has no hot corrosion problem. But in the side of economizer, there is a considerable decrease in thickness of tubes. These results are compatible with visual inspections.

Fig. 6 Presence of combustion products

Table 3 Illustration of tubes thicknesses in both sides

Tube number	Primary thickness	1	2	3	4	5	6	7	8
Smooth part thickness (mm) of tube in the economizer side	4.6	4.5	4.6	4.4	4.6	4.5	4.6	4.6	4.5
Conical part thickness (mm) of tube in the economizer side	5.6	5.6	5.5	5.4	5.5	5.6	5.6	5.5	5.4
Smooth part thickness (mm) of tube in the superheater side	4.7	4.7	4.5	4.3	4.2	4.4	4.3	4.7	4.6
Conical part thickness (mm) of tube in the superheater side	5.6	5.6	5.4	5.3	5.2	5.4	5.3	5.5	5.5

Temperature Measurements

Surveying the combustion products on the surface of generating tubes in the superheater side indicates the rise in temperature. K type thermocouples were installed on three tubes in the superheater side. Table 4 shows the temperature measurements on the surface of the tubes. Measurements of three tubes illustrate the critical conditions in terms of temperature. Therefore, it is wise to select 600 °C as the experiment temperature.

Table 4 Temperature measurements on the surface of tubes

Tube number	Thermocouple temperature (°C)	
	Without loading	Under loading (60 MV)
1	330	640
2	290	440
3	285	590

Ash XRF Analysis of the Tube Surface

Table 2 gives a breakdown of ash XRF analysis on the tube surface. Since XRF shows elements in terms of oxides, three harmful oxides (Na_2O, SO_3 and V_2O_5) totally make more than 70 wt% of ash. Although the temperature fluctuates from 600 to 1100 °C, these elements are the results of condensation at 600 °C [8] on the surface of the tubes. By calculating the molar percentage of those three oxides, it can be concluded that 25 wt% V_2O_5 is a good approximation. The amount of Na_2O is more than that is needed for the creation of Na_2SO_4. This lack can be justified by the formation of complexes of sodium vanadate. Hence, 5 wt% NaCl can balance the percentage of proposed corrosive compound in the experiments with extra amount of sodium in XRD results. Combination of Eqs. (2) and (1) can describe that some parts of NaCl change to Na_2SO_4 [19] and the rest of it forms a complex compound with V_2O_5. Although the NaCl is deposited on the surface of the tubes, the final products have no sign of Cl element [20].

$$2NaCl(s,l) + SO_2 + O_2 \rightarrow Na_2SO_4 + Cl_2 \qquad (2)$$
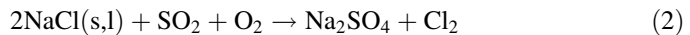
Power plant studies indicated the existence of hot corrosion in superheater side generating tubes. It is obvious that the fireside corrosion can cause mass loss or the creation of cracks which then allow failure by mechanical mechanisms such as fatigue [21]. Therefore, it will lead to other moods of failure which damage the tubes dramatically. These studies attribute selecting the temperature and corrosive deposit as two important parameters of laboratory experiments.

Burning Additive

Due to the existence of impurities when oil fuel burns, ash is produced. Chemical composition of ash highly depends on the level of O_2, SO_x, temperature and also the pressure. The main constituent of the current additive is alkyl benzene sulfonic acid with $CH_3(CH_2)_{11}C_6H_4SO_3H$ chemical formula which contains sulfur atoms. In order to understand the role of sulfonic acid in burning of magnesium sulfonate, it was burnt alone. After burning the additive at 600 °C in the air atmosphere, the ash was analyzed by XRD. The XRD result in Fig. 2 confirmed that the magnesium sulfate in dry and hydrate forms was the only mineral salt part of the ash. Consequently, magnesium sulfate was added to corrosive compound with specific ratio to make the Mg-containing compound. Formation of sulfate instead of oxide or carbonate in atmosphere pressure leads to inability of additive to absorb more sulphurous gases produced through the burning of fuel oil in power plant boilers.

Weight Loss of the Specimens

Four different Mg-containing compounds were tested. The results of weight loss are presented in Table 5 for samples coated with different Mg-containing compounds. The results indicate that the weight ratio of 3:1 for Mg to V has the highest effect in comparison with others. The higher ratio does not show a significant improvement

Table 5 Weight loss of specimens with four different Mg-containing compounds

Mg to V ratios	1:1	2:1	3:1	4:1
Weight loss (mg/cm^2) after 120 h	134	91	70	68

while it creates more ash. The result is compatible with practical advice [22], since the Mg-containing compound with ratio of 3:1 for Mg to V was selected for further studies.

Weight loss studies and physical observations were performed after doing the FESEM and XRD analyses. Figure 7 shows the appearances of specimens after passing the corrosion tests. The samples surfaces were rinsed with a smooth water flow to remove the coating compound from their surface. Specimens which have passed at least 2 cycles (or more than 48 h) with corrosive compound were damaged by pitting. The situation and surface shape of the specimens were getting worse and worse over the time because the possibility of localized pitting attacks increases over the time [23] while specimens that were coated with Mg-containing compound, there is no sign of pit and sticky corrosive compounds. So, the specimens were protected against hot corrosion. In order to perform weight loss studies, all specimens were completely removed from oxide scales to achieve the fresh metal surface. Therefore, it was possible to calculate the effect of corrosive and Mg-containing compounds on weight loss of the specimens. The weight changes were calculated by deducing the final weight of each specimen from the primary weight. The weight and metal loss diagram of both groups is presented in Fig. 8. As can be seen in Fig. 8, the rate of weight loss decreases with the time due to growing of the oxide layer. The final specimens that have passed more than 120 h at 600 °C had weight and metal loss at about 218 and 75 mg/cm^2 and 277 and 95.3 μm for the first
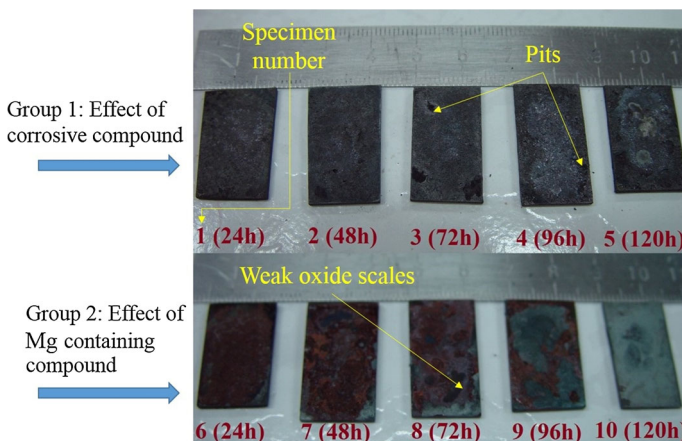

Fig. 7 Illustration of specimens under corrosive and Mg-containing compounds. The first group was coated with corrosive compound and the second with Mg-containing compound
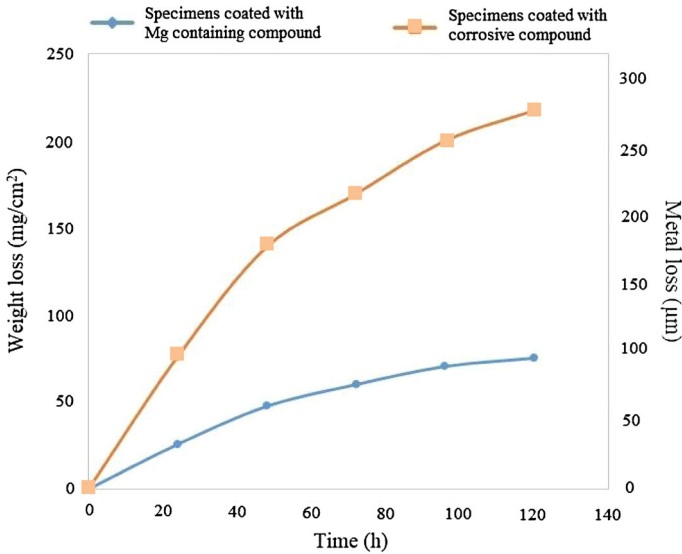
Fig. 8 Weight and metal loss diagram of both groups of specimens

and second groups of specimens, respectively. By using additive, the final weight loss was one-third of the primary statue.

Some researchers have worked on hot corrosion of steels at 600 °C, and a few of them studied the effect of magnesium additives on specimens. Barbooti et al. [4, 10] worked on effects of MgSO$_4$ and magnesium stearate on hot corrosion of steel alloys at 600 °C. Their results were similar but not the same, due to differences in corrosive compounds, alloys and the ratio of additives. It was found that increasing the additive ratio decreased the corrosion rates in their works. Selection of temperature for the test was very sensitive. Rezakhani [24] worked on rather similar corrosive compound for ferritic steels at 550 and 650 °C. The results were highly depended on the temperature and alloy compound.

Although the rate of weight loss after using additive declined considerably, it is still high for solving the power plant problem. There are some points which prove the efficiency of additive. The problem occurred when the fuel changed from natural gas to fuel oil. As it is shown in Table 4, the temperature of tubes reached to around 600 °C in loading conditions. This low carbon steel is not designed to work at this temperature. As can be seen in Fig. 9, there is a huge accumulation of corrosive ash on the surface of tubes. Due to inappropriate operation in the boiler, these sticky substances cause a problem in heat transfer. Those thick ashes layer provides surfaces that have enough temperature to create continues flow of fused salts to the surface of tube. The fused corrosive salt current leads to drop in the thickness of tubes which causes failure. Moreover, the external thickening of generating tubes restricts the space for flowing combustion gases among the tubes. This thickening

Fig. 9 Thickening of ash deposits on the surface of the tubes

will lead to increase the temperature. This effect could be justified by the results in Table 4, because the main deference between without loading and under loading conditions is the amount of combustion gases. The most important effect of additive is formation of solid ash that is not sticky; therefore, it can considerably decrease the tubes surface temperature. So that the rate of weight loss will be enormously fell down. These benefits are in addition of preventing hot corrosion.

Besides, the percentage of oxygen in the test is four times more than combustion environment. By assuming the complete prevention of hot corrosion in the test due to the lack of fused salts, the weight loss for pure oxidation of iron at 600 °C in 5% O_2 is nearly one tenth of the test value for 24 h [25]. This approximation shows that high-temperature oxidation (without hot corrosion) in combustion environment would be low enough to protect the tubes. Consequently, there would be a considerable effect after using additive in preventing tube failures.

It must be considered that during combustion with extra air (to make sure about complete combustion), sulfur in the fuel react with oxygen to create SO_2 and SO_3. This type of atmosphere is oxidizing [26]. Based on power plant information, the content of SO_2 in the stack of this boiler is <0.1%. Therefore, it could not considerably effect on Mg inhabitation [27]. Indirectly, it has an impact on corrosion through the compound of corrosive salt. As it was explained, Na_2SO_4 is the result of NaCl sulfidation.

Hot Corrosion Studies

XRD results of two final specimens 5 and 10 that were exposure at high temperature for up to 120 h are illustrated in Figs. 10 and 11, respectively. It is essential to understand the corrosion behavior of specimens before the study of inhibition effect. As it can be seen in Fig. 10, in accordance with previous studies [6, 9, 10], V_2O_5 reacts with sodium to form complex vanadate. These compounds have a relatively low melting point at about 550 °C and play a main role in hot corrosion. Despite
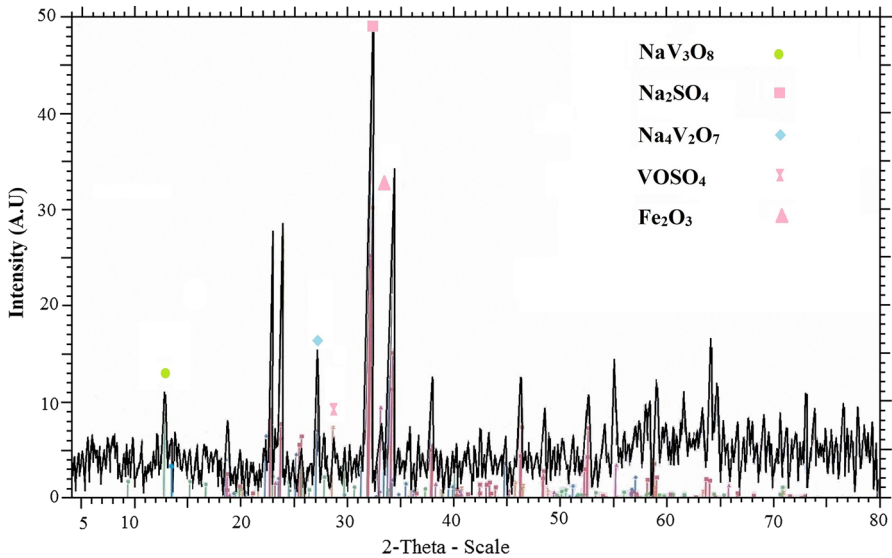
Fig. 10 XRD patterns of deposits and scales on specimen 5 coated with corrosive compound after 120 h exposure at 600 °C
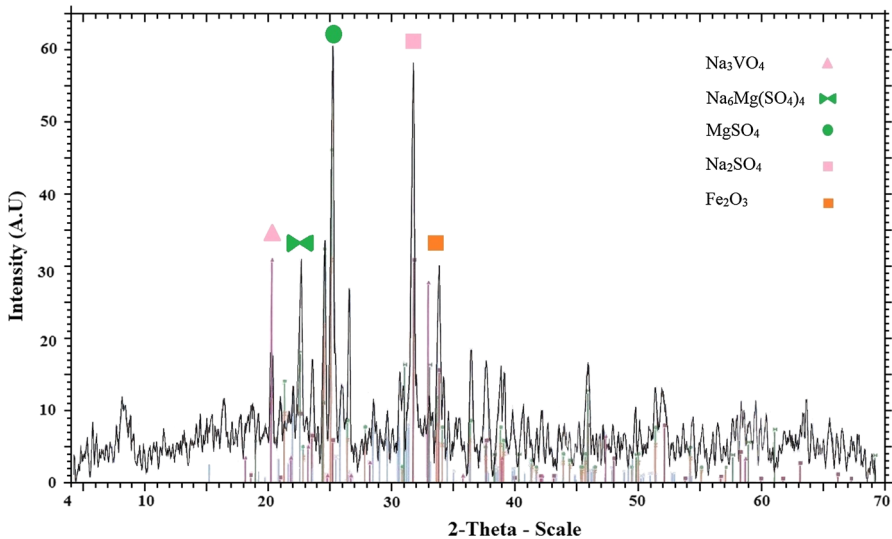

Fig. 11 XRD analysis results of deposits and scales on specimen 10 coated with Mg-containing compound after 120 h exposure at 600 °C

Na_2SO_4, V_2O_5 was completely used to form complexes of vanadate. The melting point of $VOSO_4$ [28] is 105 °C. Since fused salts are formed beneath the ash during the corrosion, it seems that two sodium vanadate compounds NaV_3O_8 and $Na_4V_2O_7$ with 548 and 603 °C melting points, respectively [1], are the main reasons for hot

corrosion in specimens. Presence of various compounds with different melting points and the local melting of these compositions confirm the pitting corrosion. It is well known that the melting point of NaCl is 800 °C and for Na_2SO_4 is 884 °C [9] and for V_2O_5 is 670 °C [6]. Therefore; in temperature of 600 °C, any of these elements in separate statue are not melted. The present results show that in regions where hot corrosion is in the form of pitting, deposits create eutectic compound which is molten in the pits. Based on phase diagram of Na_2SO_4–V_2O_5 [1], some special compounds of sodium with vanadium just have melting points below 600 °C. It seems that the mechanism of vanadium effect is the creation of molten complex, on the other hand, lowering the melting point, attributing to the oxidation diffusion, oxides solution and also increasing the acidity of flux.

It seems that formation of sufficient sodium vanadate flux on the natural cavities of Fe_2O_3 oxide layer causes the pitting of specimens (Figs. 12 and 13). At least two issues would happen in pitting regions:

1. Creation of a pit that its depth increases with low speed through enough amount of sodium vanadate flux.
2. Scaling of oxide layer around pit that is in the form of nub.

In Fig. 12 differences between deposits morphology of pit and the scale around of that are completely clear. It seems that vanadium has an important role on starting and propagation of pits. Present results in EDS analysis (in Fig. 14a, b) of Fig. 13 in point A and B confirm the above hypothesizes. Furthermore, blistering of
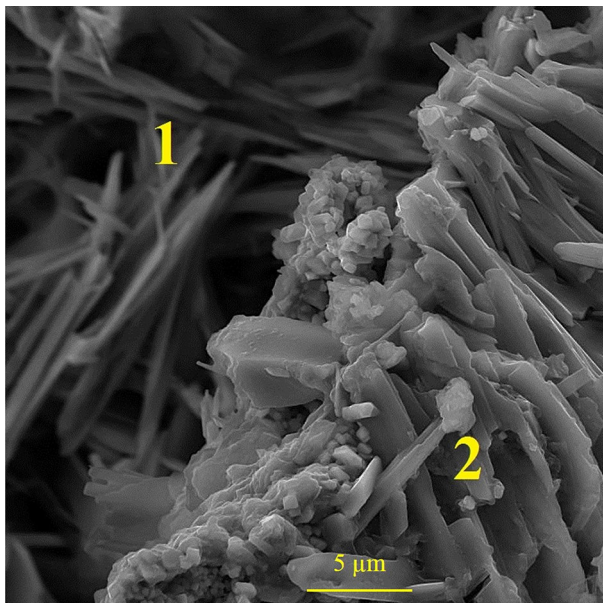

Fig. 12 Illustration of Differences between deposits morphology of pitting and scale around of that in specimen 3 after 72 h at high temperature. Regions 1 and 2 marked in the image, respectively, show inside and outside of a pit
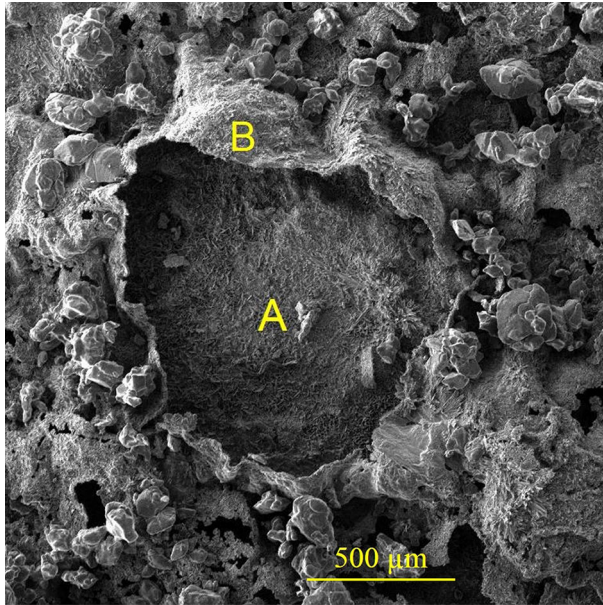
Fig. 13 Illustration of a pit and its nub region in specimen 4 after 96 h at high temperature. Regions A and B marked in the image indicate the location of EDS analysis
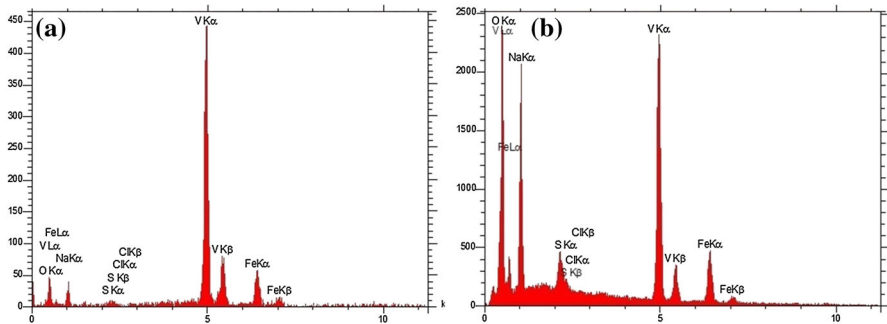

Fig. 14 EDS analysis of Fig. 13 in pit and nub region area: **a** EDS analysis of point *A* and **b** EDS analysis of point *B*

scales around pitting points more imitate through salt fluxing and weakness of scales because in weak corrosion-resistant materials, the formation of large deep pits is difficult [29]; therefore, the surface of pits propagates instead of depths. As discussed in XRD analysis, the deposit compound in Fig. 10 is containing of Na_2SO_4, $Na_4V_2O_7$, $VOSO_4$, NaV_3O_8 and Fe_2O_3. The Amount of extra Na_2SO_4 was observed in Fig. 10, but the amount of Na element in accordance with EDS analysis in Fig. 14a was less than in Fig. 14b. Therefore, there was no extra Na to be unreacted with V in pit. But highly corrosive sodium vanadate compounds were formed, which help the acidic reaction as per Eq. (1). The region around pit is rich

from Na. The problem is that the Fe_2O_3 oxide is porous and generally it is a non-protective scale [2]. Sodium vanadate goes through those defects. Because of the salt fluxing in pitting regions beneath the scale, inflation occurred. As discussed above, due to its acidic fluxing nature, in contrast with basic fluxing, acidic fluxing can be self-sustaining because the displacement of the salt from the stoichiometry does not become progressively more difficult as the reaction proceeds [30]. Linear analysis in Fig. 15 endorses that in areas where pitting started, drop in Fe and increase in vanadium contents can be seen. In other pits, such as Fig. 16, observations imitate above hypothesizes. Na is negligible which means that sodium vanadate is formed exclusively.

As it is shown in Fig. 11, the results indicate that the picks are $MgSO_4$, Na_2SO_4, $Na_6Mg(SO_4)_4$, Na_3VO_4 and Fe_2O_3. Despite inhibition mechanism that was discussed in the introduction [9], there was no sign of magnesium vanadate formation, because at this range of temperature, $MgSO_4$ does not react with V_2O_5 [5]. In contrast with chemical reactions in corrosive compound, the melting point of formed sodium vanadate (Na_3VO_4) is at about 850 °C [31]. Moreover, sodium reacts with part of magnesium to form $Na_6Mg(SO_4)_4$ at 670 °C [32]. Na_3VO_4 is a high melting point sodium vanadate salt, in comparison with $Na_4V_2O_7$ and NaV_3O_8. Sodium vanadate salts are very harmful for hot corrosion resistance when they are fused at test temperature. Concurrently, there will be no fused part to be separated from ash and flux through oxide scales and produce nub region. So, the mechanism of inhibition is formation of Na_3VO_4 as a harmless sodium vanadate that is solid at 600 °C instead of liquid $Na_4V_2O_7$ and NaV_3O_8. Formation of sodium vanadate salts is very complex. Therefore, it seems that existence of $MgSO_4$ in Mg-containing compound at 600 °C changes the chemical reactions between Na_2SO_4 and V_2O_5. As it is shown in Fig. 17, the morphology of Mg-containing compound is not affected by molten salts and therefore ash products are not solidified and stuck to the surface of the specimens.

It can be concluded from different research [4, 5, 12] that chemical reaction between salts on the surface of metals at high temperature is just depended on the
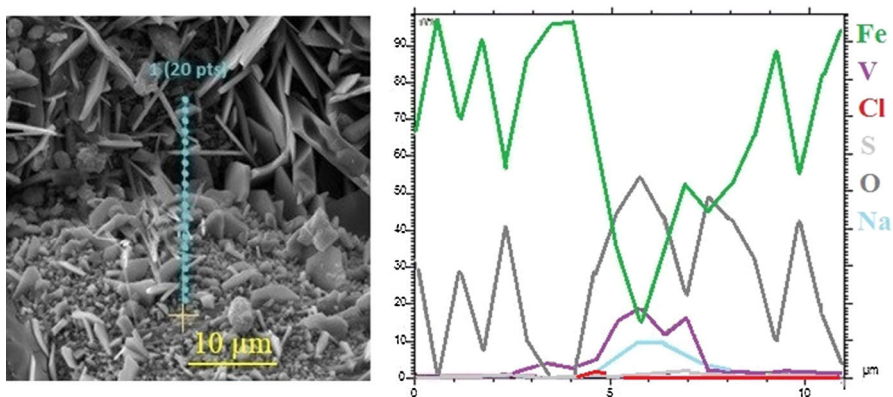

Fig. 15 Illustration of chemical composition changes in boundary of pit by using linear analysis scan of specimen 4 after 96 h at high temperature
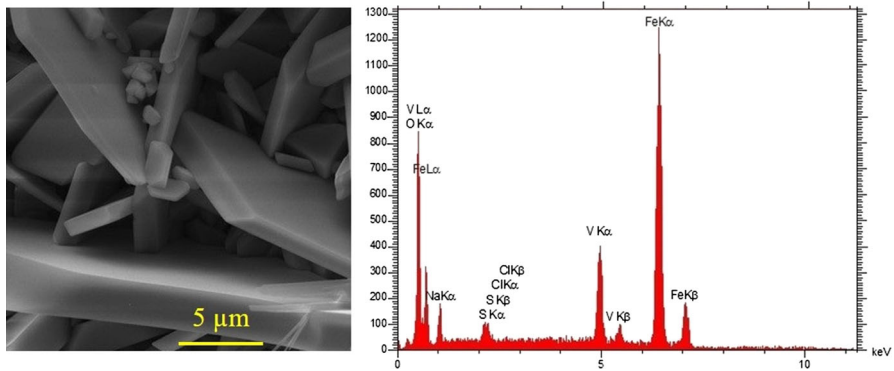
Fig. 16 High magnifying of a pit with its EDS analysis in specimen 4 after 96 h at high temperature which indicate the lowering Na against V in pit
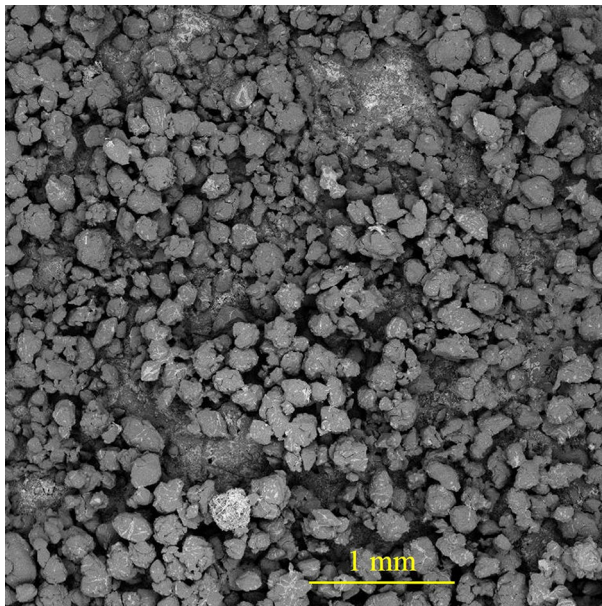

Fig. 17 Morphology of Mg-containing compound (Not melted compounds containing Na_3VO_4, $Na_6Mg(SO_4)_4$, $MgSO_4$ and Na_2SO_4)

temperature and not to time. Therefore, the minimum time of test (24 h) is enough to reach a stable condition for surface reactions.

Figures 18 and 19 show the cross sections of the specimens coated with corrosive and Mg-containing compounds, respectively. Based on EDS analysis in Fig. 18, it is obvious that corrosive compounds are fused and go through the beneath of scales. It seems the harmful effect of corrosive salts is not only accelerating high-temperature oxidation but also the spallation of substrate like an internal attack. As it is shown in
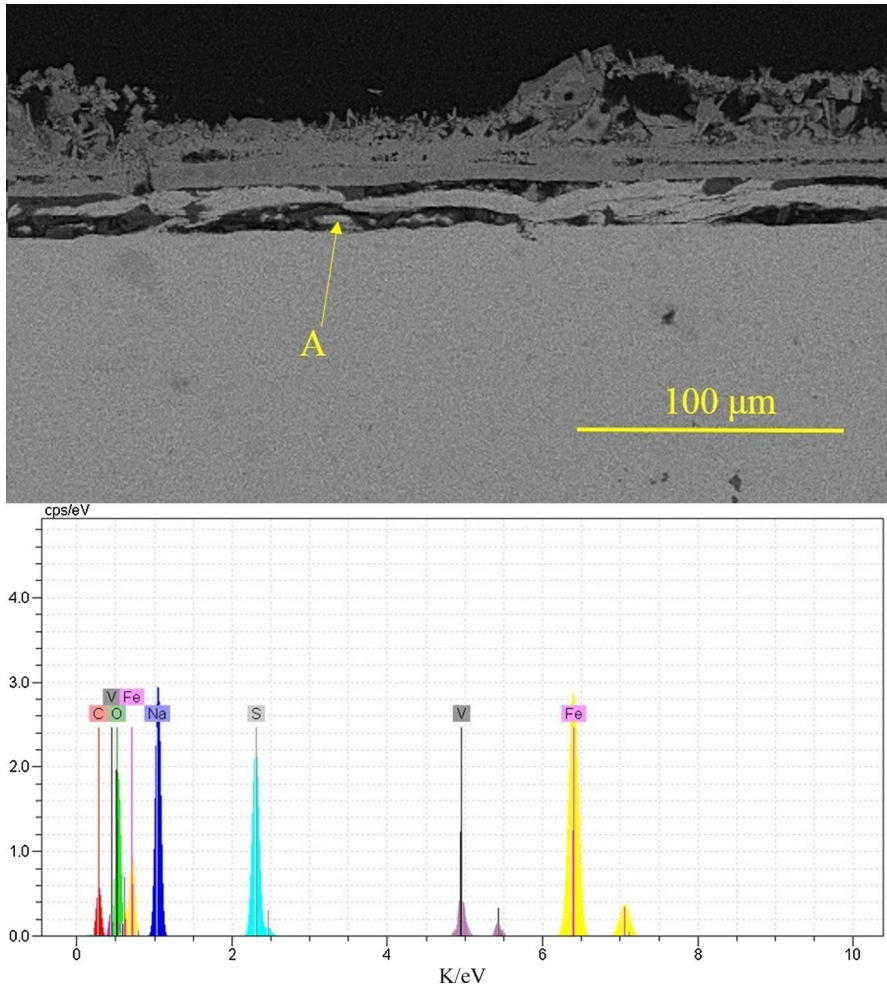
Fig. 18 Cross section of specimen 5 after 120 h at high temperature and EDS analysis beneath a blistered point

Fig. 18, the general shape of substrate layer in Mg-containing compound is better than that of Fig. 17. EDS analysis in Fig. 18 does not show any sign of corrosive compounds. It looks all the salts were in solid state during the test and there was no sign of fused salts. The schematic illustration of hot corrosion and inhibition of specimens are shown in Fig. 20. As can be seen in the corrosive containing compound, the fused salts of sodium vanadate go through oxide layer cavities while in the Mg-containing compound the solid sodium vanadate stays in the surface. It must be noticed that most of deposit-induced accelerated attack occur when the deposit is a liquid, although some examples of attack caused by solid deposits are available [23]. Solid deposits are corrosive when they can react with scales [33], but XRD results do not show any reaction between deposits and Fe_2O_3.
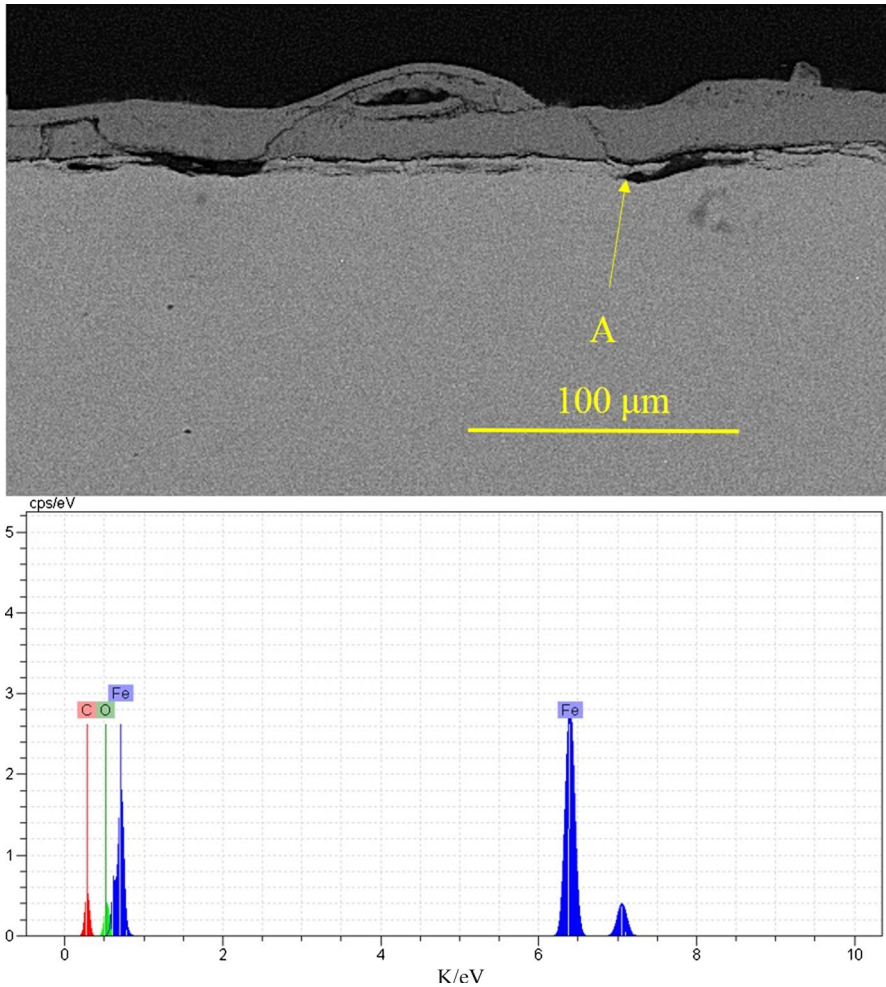
Fig. 19 Cross section of specimen 10 after 120 h at high temperature and EDS analysis beneath a Mg-containing compound

Hence in this condition, protection occurred when deposits are solids. Therefore, magnesium sulfonate can be suggested to the power plants to use for the short periods of time that the fuel type is changed.

Conclusions

The high-temperature corrosion behavior of low carbon steel and inhibition of magnesium sulfonate was studied. The following conclusions can be drawn:

1. Magnesium sulfonate is an effective hot corrosion inhibitor but cannot reduce the emission of sulphurous gases in power plant boilers.
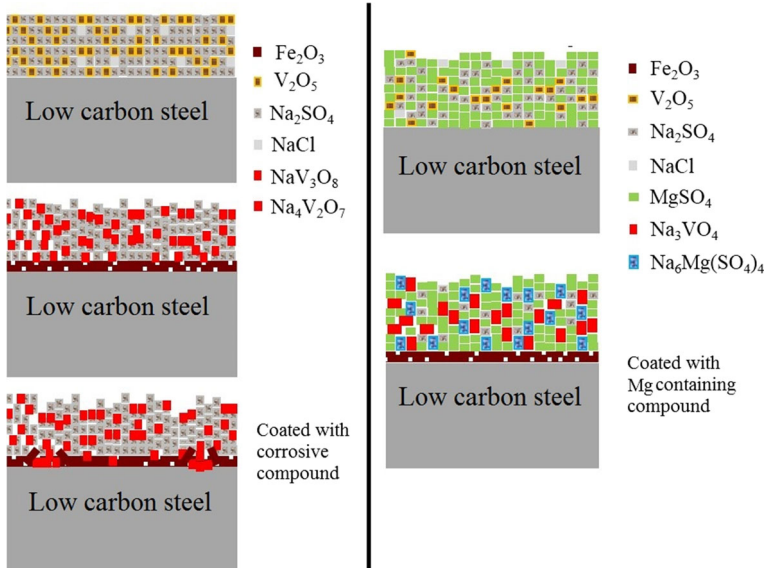
Fig. 20 Schematic illustration of hot corrosion and inhibition of specimens

2. By using additive, specimens were protected against hot corrosion, but in the corrosive containing compound, corrosion in the form of pitting was clear. The optimum additive ratio of Mg to V was 3:1.
3. By using additive, the weight loss after 120 h was decreased from at about 218–75 mg/cm^2.
4. Surface and cross-sectional studies show that S, Na and V are key elements of corrosion, but in points where Na is low in comparison with Vanadium, it seems that the creation of sodium vanadate molten flux is the most important reason of pits propagation.
5. The Formation of sodium vanadate salts is very complex. So, it seems that existence of $MgSO_4$ in Mg-containing compound at 600 °C changes the chemical reactions between Na_2SO_4 and V_2O_5. The mechanism of inhibition is formation of Na_3VO_4 as a harmless sodium vanadate that is solid at 600 °C instead of $Na_4V_2O_7$ and NaV_3O_8 that are liquid at this temperature.

References

1. H. Singh, and D. Puri, *Review Advanced Material Science* **16**, 27 (2007).
2. G. Kaushal, H. Singh, and S. Prakash, *Oxidation of Metals* **76**, 169 (2011).
3. J. Barroso, F. Barreras, and J. Ballester, *Fuel Processing Technology* **86**, 89 (2004).
4. M. M. Barbooti, S. A. Al-Niaimi, and K. F. Al-Sultani, *Material and Environmental Science* **36**, 686 (2012).

5. J. L. Tristancho-Reyes, J. G. Chacón-Nava, D. Y. Peña-Ballesteros, C. Gaona-Tiburcio, et al., *Electrochemistry Science* **6**, 432 (2011).
6. I. Andijani and AU. Malik, Riyadh. 11 to 15 Dec (2004).
7. C. C. Arteaga, J. U. Chavarín, J. P. Calderon, G. I. Montalvo, J. Gonzalez, et al., *Corrosion Science* **46**, 2663 (2004).
8. N. Otsuka, *Corrosion Science* **44**, 265 (2002).
9. Y. K. Afifi, A. F. Waheed, and S. W. Sharkawy, HEB 97, Alex andria. Egypt; April (1997).
10. M. M. Barbooti, S. H. Al-Madfai, and H. J. Nassouri, *Thermochemical Acta* **126**, 43 (1988).
11. G. H. Meier, *Materials Science and Engineering* **120**, 1 (1989).
12. J. G. Gonzalez-Rodriguez, S. Haro, A. Martinez-Villafãne, V. M. Salinas-Bravo, and J. Porcayo-Calderon, *Materials Science and Engineering A* **435–436**, 258 (2006).
13. N. K. Mishra, A. K. Rai, S. B. Mishra, and R. Kumar, *International Journal of Corrosion* **2014**, 453607 (2014).
14. E. Kaufman, GER-3764A. General Electric Company (1996).
15. B. Buecker, *Basics of Boiler and HRSG Design*, (PennWell, Tusla, Oklahoma, 2002).
16. R. D. Charles and M. W. Paul, inventors; Bray Oil Company, Assignee. Overbased Magnesium Sulfonate Process. US patent 4,192,758.
17. M. F. Ali, and S. Abbas, *Fuel Processing Technology* **87**, 573 (2006).
18. A. Ajay, V. S. Raja, G. Sivakumar, and S. V. Joshi, *Corrosion Science* **98**, 271 (2015).
19. F. Pettit, *Oxidation of Metals* **76**, 1 (2011).
20. S. Lee, *Journal of Thermal Spray Technology* **16**, 1 (2007).
21. B. S. Lutz, G. R. Holcomb, and G. H. Meier, *Oxidation of Metals* **84**, 353 (2015).
22. E. George, *Totten, Fuels and Lubricants Handbook: Technology, Properties, Performance, and Testing*, (ASTM International, West Conshohocken, Pennsylvania, 2003).
23. A. A. Khadom, H. Liu, A. A. Fadhil and A. M. A. Karim, *Oxidation of Metals* **86**, 553 (2016).
24. D. Rezakhani, *Anti-Corrosion Methods and Materials* **54**, 237 (2007).
25. B. Pujilaksono, T. Jonsson, M. Halvarsson, J. E. Svensson and L. G. Johansson, *Corrosion Science* **52**, 1560 (2010).
26. G. Y. Lai, *High-Temperature Corrosion and Materials Applications*, (ASM International, West Conshohocken, 2007).
27. T. N. Rhys-Jones, J. R. Nicholls and P. Hancoock, *Corrosion Science* **23**, 139 (1983).
28. http://www.sigmaaldrich.com/catalog/product/aldrich/204862?lang=en&region=IR.
29. Y. Kawahara, *Oxidation of Metals* **85**, 127 (2016).
30. J. Stringer, *Materials Science and Technology* **3**, 482 (1987).
31. M. Molière and J. Sire, *De Physique III* **3**, 719 (1993).
32. Jr. Meskers, A. Donald, M. Michel, B. Jeanluc inventors; Jr. Meskers, A. Donald, M. Michel, B. Jeanluc, Assignee. Method of Operating a Combustion Installation and Use of Such a Method for Inhibiting Vanadium Corrosion. US patent 20130213282.
33. K. Y. Jung, F. S. Pettit and G. H. Meier, *Materials Science Forum* **595–598**, 805 (2008).